Water Research 169 (2020) 115217

Contents lists available at ScienceDirect

Water Research

journal homepage: www.elsevier.com/locate/watres

The concentrations and characteristics of dissolved organic matter in high-latitude lakes determine its ambient reducing capacity

Tao Jiang [a, b, *], Dingyong Wang [a, b], Bo Meng [c], Jinshu Chi [b], Hjalmar Laudon [b], Jiang Liu [a, d]

[a] State Cultivation Base of Eco-agriculture for Southwest Mountainous Land, Department of Environmental Sciences and Engineering, College of Resources and Environment, Southwest University, Chongqing, 400716, China
[b] Department of Forest Ecology and Management, Swedish University of Agricultural Sciences, Umeå, SE-90183, Sweden
[c] State Key Laboratory of Environmental Geochemistry, Institute of Geochemistry, Chinese Academy of Sciences, Guiyang, 550002, China
[d] Centre for Earth Observation Science, Department of Environment and Geography, University of Manitoba, Winnipeg, MB R3T 2N2, Canada

ARTICLE INFO

Article history:
Received 10 July 2019
Received in revised form
16 October 2019
Accepted 18 October 2019
Available online 19 October 2019

Keywords:
Arctic
Ambient reducing capacity
Dissolved organic matter
Electron donation capacity
Mercury
Lakes

ABSTRACT

The reducing capacity (RC) of natural organic matter plays an important role in the carbon cycle and biogeochemical fates of environmental contaminants in the aquatic system. However, the electron donation potentials of dissolved organic matter (DOM) from high-latitude lakes are still uncertain. In this study, we collected DOM samples from high-latitude lakes across the Arctic and boreal regions in Sweden and Norway to investigate the effects of the DOM concentration and characteristics on its ambient reducing capacity (ARC). Mercury (Hg(II)) abiotic reduction in darkness was used to determine the ARC. The results showed that the DOM in Arctic lakes is less terrestrial-dominant than in reference sites (i.e., forest lakes). Between the two categories of Arctic lakes, tundra lakes are more terrestrial-influenced compared to mountain lakes. Additionally, terrestrial-originated DOM is a main controlling factor for enhancing the ambient reducing capacity, whereas the DOM concentration, i.e., dissolved organic carbon (DOC), resulted in variations in the Hg/DOC ratios that also cause the variations of the observed ARC values. Thus, comparisons of the ARC values can be conducted while oxidant/DOC ratios are kept the same and reported through the method using heavy metals as a chemical probe. After correction for Hg/DOC ratio interference, the ambient reducing capacity of DOM followed the order: boreal forest lakes > Arctic tundra lakes > Arctic mountain lakes. This study highlights that the DOM concentration should also be considered when estimating the ARC as compared to the previous that mainly focusing on the properties of DOM such as its origins. As climate change is projected to be severe in high latitudes, this study demonstrates a significant connection between aquatic DOM geochemical reactivity and terrestrial inputs, which is crucial for a better prediction of the role of DOM in high-latitude lakes in the context of climate change.

1. Introduction

The high-latitude lakes, in particular those in the Arctic regions, are currently experiencing rapid changes due to climate warming (Cory et al., 2013, 2014; Osburn et al., 2017), which act as a potential source of greenhouse gases such as CO_2 and CH_4 (Schuur et al., 2015; O'Donnell et al., 2016). Ongoing climate change has resulted in the permafrost thawing, which can promote the release of carbon previously stored in terrestrial systems (Vonk et al., 2015) into adjacent lakes. During the past decades, several studies have qualitatively and quantitatively addressed various aspects of dissolved organic matter (DOM) in Arctic rivers (Cory et al., 2014; O'Donnell et al., 2016; Kaiser et al., 2017), lakes (Cory et al., 2014;

Abbreviations: ARC, Ambient reducing capacity; BIX, Biological index; CDOM, Chromophoric dissolved organic matter; CVAAS, Cold vapor atomic absorption spectroscopy; DOC, Dissolved organic carbon; DOM, Dissolved organic matter; EEMs, Emission-Excitation matrices; FI, Fluorescence index; Hg, Mercury; HIX, Humification index; IHSS, International society of humic substances; NOM, Natural organic matter; OM, Organic matter; RC, Reducing capacity; RFE, Relative fluorescence efficiency; S_R, Spectral slope ratio; SUVA, Specific ultraviolet absorbance; UV–Vis, Ultraviolet–visible.

* Corresponding author. State Cultivation Base of Eco-agriculture for Southwest Mountainous Land, Department of Environmental Sciences and Engineering, College of Resources and Environment, Southwest University, Chongqing, 400716, China.

E-mail address: jiangtower666@163.com (T. Jiang).

https://doi.org/10.1016/j.watres.2019.115217
0043-1354/

Osburn et al., 2017) and oceans (Shen et al., 2016; Mann et al., 2016) and reported that terrigenous DOM is abundant and widely distributed in Arctic surface waters. The internal links between the carbon cycle resulting from DOM bio-/photodegradation and DOM quality have also been explicitly established (Cory et al., 2013, 2014; Larouche et al., 2015; Kaiser et al., 2017). However, there have been fewer studies to assess the relationships between DOM properties (e.g., origins) and its biogeochemical reactivities (e.g., reducing capacity) in these areas, as compared with other studies in low-latitude aquatic systems. Investigation of the origins, characteristics, and biogeochemical reactivities of DOM in such regions is therefore crucial for a further understanding of the regional carbon dynamics (Karlsson and Giesler, 2008; Cory et al., 2013, 2014; Kokic et al., 2015) and the relevant environmental fates of contaminants in the Arctic environment (Wei-Hass et al., 2014; Schartup et al., 2015a; Jonsson et al., 2017).

Among all of biogeochemical reactivities of DOM, the redox characteristics play an important role not only in the production of CO_2 and CH_4 (Blodau et al., 2007; Knorr and Blodau, 2009; Gao et al., 2019) but also in the chemical speciation, bioavailability, toxicity, and mobility of various elements and contaminants in aquatic systems. For example, the electron-donating transfer ability of DOM facilitates the reduction of many elements such as sulfur (S) (Yu et al., 2015; Poulin et al., 2017), iron (Fe) (Lovley et al., 1996, Lovley and Blunt-Harris, 1999; Scott et al., 1998; Kappler et al., 2004; Peretyazhko and Sposito, 2006; Jiang and Kappler, 2008), and copper (Cu) (Pham et al., 2012; Maurer et al., 2013) as well as the reduction of redox-sensitive trace heavy elements and even radionuclides such as chromium (Cr) (Gu and Chen, 2003), mercury (Hg) (Gu et al., 2011; Zheng et al., 2012; Jiang et al., 2015), uranium (U) (Gu and Chen, 2003; Gu et al., 2005) and neptunium (Np) (Shcherbina et al., 2007). Reductive degradation of organic contaminants could also be mediated by DOM (Kappler and Haderlein, 2003). Thus, determining the electron transfer potential of DOM is a key step to understand its crucial roles in diverse environments.

Quantitatively, the electron donation capacity of natural organic matter (NOM), also called the reducing capacity (RC), is defined as the moles of electrons that can be donated or transferred by the per-unit amount of NOM (e.g., normalized carbon amount). To date, extensive studies have been carried out to assess the reducing capacities of DOM, with a wide range of values reported depending on varying quantification methods and NOM origins (Macalady and Walton-Day, 2011; Sposito, 2011). It remains a major challenge to accurately determine the reducing capacity or reflect the relevant environments. Typically, two types of methods have been widely used in parallel in the past (1) the chemical probe method (i.e., wet chemical method) (Lovley et al., 1996; Scott et al., 1998; Kappler et al., 2004; Peretyazhko and Sposito, 2006; Jiang and Kappler, 2008): and (2) the electrochemical method (Aeschbacher et al., 2010, 2012; Nurmi and Tratnyek, 2011). There is an argument about the advantages and disadvantages of these two methods. Although the chemical probe method is a traditional approach that relies on reaction with added chemical oxidants, such as the Fe(III) species (Kappler et al., 2004; Peretyazhko and Sposito, 2006; Bauer et al., 2007; Roden et al., 2010), it may result less accuracy than the electrochemical method due to indirect measurement and poorly controlled experimental conditions (e.g., E_H) (Aeschbacher et al., 2010; Gao et al., 2019). However, it has a unique advantage that it can reflect the kinetic and thermodynamic processes involving the complexation (e.g., rearrangement of binding sites) between target contaminants and DOM structures (i.e., binding groups and electron transfer moieties) (Shcherbina et al., 2007; Gu et al., 2011; Pham et al., 2012; Zheng et al., 2012; Jiang et al., 2015) if the study aims to study a specific contaminant, especially trace heavy metals (e.g., Hg). Thus, the electrochemical method cannot replace the chemical probe method, especially in less well-equipped laboratories and in-field analyses (Macalady and Walton-Day, 2011).

The most popular and widely used chemical probes in the previous studies are ferric compounds, such as ferric citrate (Lovley et al., 1996, Lovley and Blunt-Harris, 1999; Scott et al., 1998; Peretyazhko and Sposito, 2006) and hexacyanoferrate (Helburn and MacCarthy, 1994; Kappler and Haderlein, 2003; Kappler et al., 2004; Jiang and Kappler, 2008), where Fe(II) was quantified by a ferrozine assay (Stookey, 1970; Viollier et al., 2000). The reducing capacity is usually calculated by quantifying the electrons transferring from organic matter to Fe(III) while forming Fe(II). Traditionally, this iron-test method requires manipulation of bulk DOM first, including DOC dilution, pH adjustment, buffer addition, or even pre-reduction. Thus, the reducing capacity is more likely an operational parameter, which is slightly far from that of the real environment, especially in high DOC conditions. For example, DOM in the sediment of pore water shows a reducing capacity for Hg(II) after dilution in the laboratory; however, we found the contribution of electrons from DOM was negligible due to the high DOC in the real environment (Jiang et al., 2018b). Additionally, as DOM is an operational definition of water mixtures, water chemistry (e.g., inorganic background such as the pH) influences its properties and further results in a changed biogeochemical reactivity. Thereby, DOM should be considered as a system in which organic components are predominant but within the specific steric structures under the ambient inorganic backgrounds (Kothawala et al., 2014). Thus, we proposed the parameter of the ambient (i.e., apparent) reducing capacity (ARC) as a further supplement for the chemical probe methods according to the proposed concept of the NOM reducing capacity from the pioneering works by Kappler and Sposito (Kappler et al., 2004; Peretyazhko and Sposito, 2006; Sposito, 2011).

The ambient reducing capacity can be directly obtained from the original DOM samples (without manipulation) by using the chemical probe method, representing the specific reducing capacity of DOM in an ambient environment. Especially, regarding the samples with high DOC concentrations for determining the ARC, traditional colorimetry in the iron-test method has limitations due to the complexation of Fe(III)/Fe(II) with DOM (Viollier et al., 2000; Poulin et al., 2014) and influence of chromophoric DOM (CDOM) (Xiao et al., 2013, 2015). Alternatively, we selected the Hg abiotic reduction in dark conditions (Alberts et al., 1974; Allard and Arsenie, 1991; Gu et al., 2011; Zheng et al., 2012; Jiang et al., 2014, 2015; Lee et al., 2019) to determine the ARC of dissolved organic matter, hereafter the ARC_{Hg}. One of the advantages of Hg(II) reduction is that Hg is a unique heavy metal element that has a gaseous phase (i.e., Hg(0)), which can be continuously purged into robust oxidizing solution (e.g., $KMnO_4$ or aqua regia) or a gold-coated glass trap for further independently measuring the Hg(II). Compared to the iron-test, the reduction of Hg(II) avoids interferences from the further interaction between the reductive product and DOM in the system. Additionally, measurement of the trapped Hg(II) is conducted by cold-vapor fluorescence or an absorption method instead of colorimetry, which is independent of the reduction system containing DOM and thus avoids the influences of chromophoric DOM.

Previous studies of humic or soil organic matter illustrated higher reducing capacity is associated with higher aromaticity derived allochthonous sources (Macalady and Walton-Day, 2011), therefore, we hypothesized that DOM from lakes with higher terrestrial inputs (e.g., forest lakes) shows higher electron donation capacities. DOM samples were collected from 29 northern lakes situated across a latitude gradient from 67.3 to 69.3°N in Sweden and Norway (i.e., above the Arctic circle), and further extending to the boreal region of Sweden as a reference (63.6–64.3°N). To

address the knowledge gaps as all mentioned above, the main aims of this study were three-fold: (1) to characterize the properties and origins of DOM in the Arctic lakes; (2) to quantify the ARC of dissolved organic matter using the Hg(II) reduction method; and (3) evaluate the influences of DOM origins and properties on its ARC.

2. Materials and methods

2.1. Sampling strategy

Generally, the origins of lake DOM consist of both autochthonous (i.e., produced in the lake such as microbial and algae) and allochthonous (i.e., external inputs such as terrestrial runoff or leaching), which are dependent on the specific environmental conditions, including catchment characteristics and climate (Sobek et al., 2007; Kothawala et al., 2014; Larson et al., 2014; Jiang et al., 2018a, b). The DOM samples were collected from 29 high-latitude lakes in the Arctic and boreal areas from Andenes (Norway) to Abisko (Sweden) and then finally to Umeå of Sweden (Fig. 1). According to the surrounding landscapes, we divided the 29 lakes into three categories, including tundra, mountain, and boreal forest lakes, respectively (Fig. 1). The nine lakes investigated in Norway are Arctic tundra lakes ($n = 9$) within the permafrost tundra landscapes partially mixed with dwarf shrubs, mire, and peatland. Arctic mountain lakes ($n = 10$) are thermokarst lakes, surrounded by mosses, lichens, and dwarf shrubs. Ten boreal forest lakes ($n = 10$) are located in northern Sweden within the boreal forest landscapes, and the dominant tree species include Scots pine, Norway spruces, and some birch.

All water samples of Arctic lakes were collected during the summer of 2018 (July to August). Boreal forest lakes were sampled from May to June of 2018. Samples were collected ~30 cm below the surface water in a well-mixed location and syringe-filtered *in situ* using a 0.45 μm (cellulose acetate membrane) filter (Sarstedt®, Germany). Two parameters of the water, including the pH and conductivity, were measured *in situ* using the pH/conductivity portable combo-meter (HI-98129, HANNA®, Italy). A part of the original water sample (0.5–1 L) was kept intact as backup storage. All samples were stored in the dark and kept in ice storage boxes during the sampling campaign and transportation, and they were stored in the 4 °C low-temperature storage room before analysis.

2.2. DOM property analysis

2.2.1. DOM characterization

The DOM concentration (represented by dissolved organic

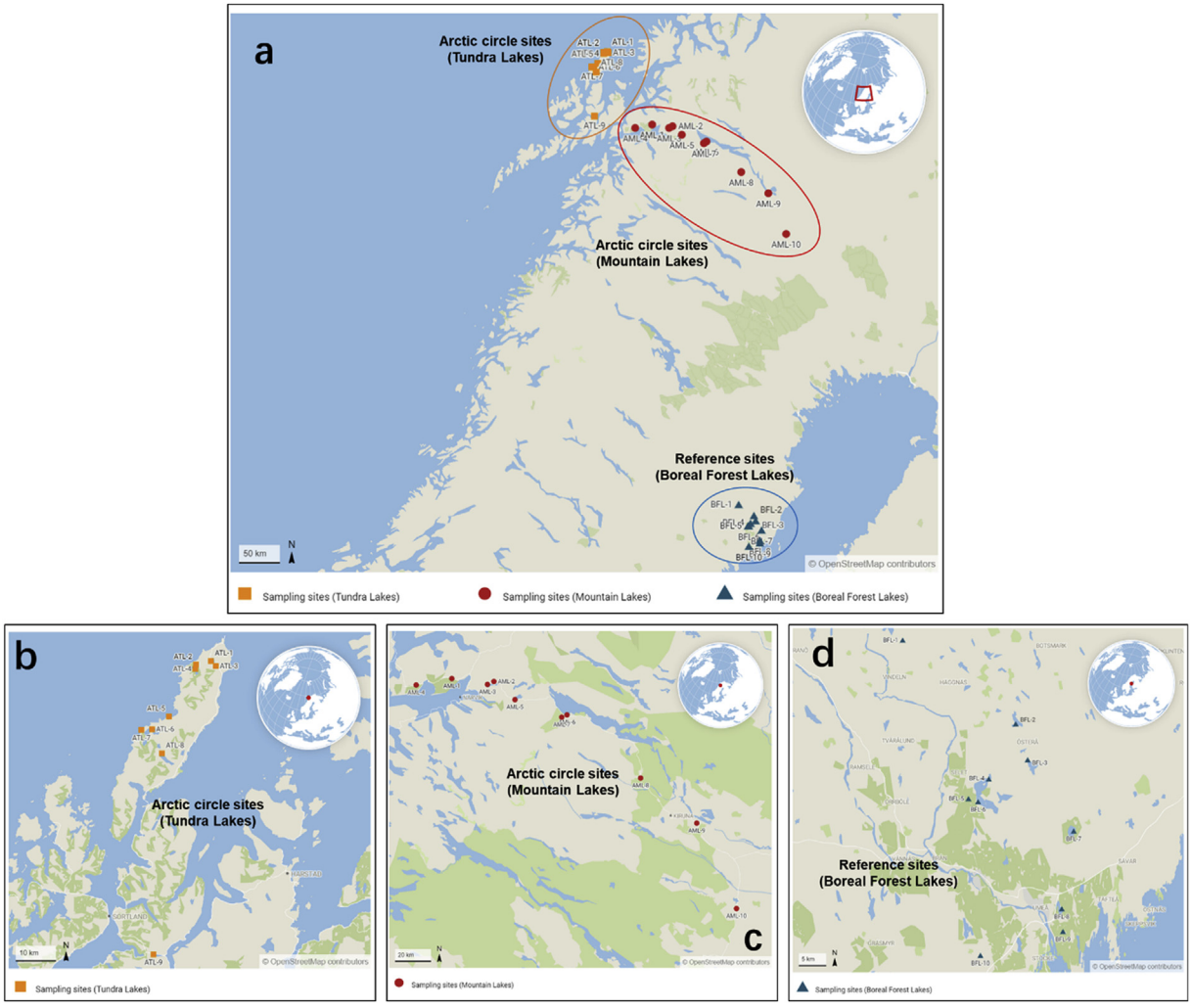

Fig. 1. Sampling sites of this study including Arctic lake sites in Norway and Sweden as well as reference sites (i.e., boreal forest lakes) in southern Sweden out of the Arctic circle (a). Three categories of lakes based on the surrounding landscapes and elevations were defined including Arctic tundra lakes ($n = 9$) (b), Arctic mountain lakes ($n = 10$) (c), and boreal forest lakes ($n = 10$) (d) as the reference.

carbon (DOC)) and total nitrogen (TN) were measured using a TOC analyzer (TOC-V, Shimadzu, Japan), as represented by the dissolved organic carbon (DOC) ($mg \cdot L^{-1}$). Additionally, we measured the nitrate (NO_3^-) and ammonium (NH_4^+) using ion-selective electrodes (Bante Instrument Shanghai, China) and subtracted them from the TN to obtain the dissolved organic nitrogen (DON). The nitrogen/carbon molar ratio (i.e., N/C) was calculated as the DON/DOC.

For optical characterization of the DOM, fluorescence and UV−vis measurements were conducted in a 10 mm quartz cuvette using an Aqualog® (Horiba, Japan) absorption-fluorescence spectroscopy instrument equipped with a 150 W ozone-free xenon lamp at constant room temperature (20 °C). For emission-excitation matrices (EEMs) of the fluorescence spectra scan, Milli-Q® water (18.2 M•cm) was used as a blank to be subtracted from sample EEMs to remove the interferences of water Raman peaks. EEMs were corrected for the inner filter effect using the parallel absorbance measurements from the same sample and blank (Yang and Hur, 2014) using the Aqualog® EEMs data processing software, which also adjusted the instrument-specific excitation and emission effects. These corrections were also double-checked using OriginPro® 2017. The emission spectral range was 250−620 nm in 3.18 nm steps, and the excitation spectral range was 230−450 nm with steps of 5 nm. The scan integration time was 3 s. The UV−vis scan ranged from 230 to 800 nm with a 1 nm interval. Milli-Q® water was used as the blank. The Naperian absorption coefficient (a) at wavelength λ (nm) was calculated as:

$$a(\lambda) = 2.303^{*}A/l \quad (1)$$

where A is the absorbance and l is the cuvette path length (m).

The fraction of DOM having light-absorbing properties, called chromophoric DOM (CDOM), is an important means of quantifying the pool of DOM. The absorption coefficient at 355 nm ($a(355)$) was chosen to represent the quantity of CDOM (Jiang et al., 2018b). The DOM samples with high DOC concentrations (e.g., samples from boreal forest lakes) were diluted to DOC < 10 mg L^{-1} before all spectra scanning (including absorption and fluorescence) to avoid the inner filter effect. Thus, the original abundance of CDOM reported in this study was calculated by multiplying the measured values by the dilution factor.

2.2.2. DOM spectral parameters and the two end-member mixing model

After iron correction, the specific UV absorbance at 254 nm ($SUVA_{254}$) associated with DOM aromaticity and humification was calculated as A_{254} normalized by the DOC concentration (Weishaar et al., 2003). In both wavelength ranges (275−295 nm and 350−400 nm), the spectral slope (S) of the DOM absorption curve was fitted by a nonlinear regression using Eq (2):

$$a(\lambda) = a(\lambda_r)^{*}\exp[-S(\lambda-\lambda_r)] \quad (2)$$

where λ_r is a reference wavelength. Moreover, the spectral slope ratio (S_R) was calculated by Eq (3) (Helms et al., 2008):

$$S_R = S_{275\text{-}295}/S_{350\text{-}400} \quad (3)$$

Through fluorescence analysis, for distinguishing DOM sources, the fluorescence index (FI) was calculated as the ratio of the fluorescence intensities at the emission wavelengths of 450 and 500 nm (excitation wavelength was kept at 370 nm) (McKnight et al., 2001; Huguet et al., 2009).

Additionally, the biological index (BIX), an indicator of the newly produced DOM from microbial/algae origins (i.e., autochthonous inputs), also called the freshness index, was calculated as the ratio of the emission intensity at 380 nm to the emission intensity of the maximum value in the range of 420−435 nm with excitation at 310 nm (Wilson and Xenopoulos, 2009; Fellman et al., 2010). The relative fluorescence efficiency (RFE) was calculated by the fluorescence intensity at an excitation wavelength of 370 nm and emission wavelength of 460 nm divided by the absorbance at 370 nm, which represents the relative amounts of algal and non-algal moieties of DOM (Downing et al., 2009; Hansen et al., 2016).

For further tracking the DOM origins as a cross-validation, we also used the mixing model of the nitrogen/carbon ratio to estimate the fractions of terrestrial (i.e., allochthonous) and non-terrestrial (i.e., autochthonous) contributions to the DOM (Perdue and Koprivnjak, 2007; Jiang et al., 2018b):

$$f_{allo} = \frac{\left(\frac{N}{C}\right) - \left(\frac{N}{C}\right)_{auto}}{\left(\frac{N}{C}\right)_{allo} - \left(\frac{N}{C}\right)_{auto}} \times 100\% \quad (4)$$

$$f_{auto} = \frac{\left(\frac{N}{C}\right)_{allo} - \left(\frac{N}{C}\right)}{\left(\frac{N}{C}\right)_{allo} - \left(\frac{N}{C}\right)_{auto}} \times 100\% \quad (5)$$

where f_{allo} and f_{auto} represent the percentage fractions (%) of organic matter from the allochthonous and autochthonous sources, respectively, and $(N/C)_{allo}$ and $(N/C)_{auto}$ are for the two end-members including the allochthonousness (0.01) and autochthonousness (0.1), respectively (Perdue and Koprivnjak, 2007; Jiang et al., 2018b).

2.3. Determination of the ARC_{Hg} by Hg(II) abiotic reduction assays

2.3.1. Reduction kinetic experimental set-up

A continuously purging incubation system was established for the Hg(II) abiotic reduction assays (Fig. 2), following the setup described in our previous works (Jiang et al., 2014, 2015; Zhu et al., 2018). Kinetic experiments were conducted with 7 time intervals: 10 min, 30 min, 2 h, 6 h, 24 h, 48 h, and 72 h. Eight systems mainly consisted of three components, including reaction, washing, and trap units that are borosilicate bottles. Reaction units with Teflon® caps containing Hg(II) and DOM were wrapped with aluminum foil and kept in the dark throughout the entire experimental period. Reaction and trap solutions were both continuously mixed using a Teflon® magnetic bar and a magnetic stirrer (Topolino®, IKA). The speed of the magnetic bar was adjusted to ~25 rpm to obtaining a steady vortex on the solution surface. All units in this system were connected by Teflon® tubes. We set two experimental conditions to determine the ambient reducing capacity: (1) same Hg addition with varying Hg/DOC mass ratios and (2) same Hg/DOC mass ratio within varying Hg additions.

The experimental conduction procedures have been described in detail in Jiang et al. (2014, 2015) and Zhu et al. (2018). In brief, high-purity N_2 gas (>99.99%) (AGA®, Sweden) was introduced ($0.2\ L\ min^{-1}$) continuously into the system through all of the units to transport the Hg(0) produced by a reduction in the reaction unit. The washing unit containing cysteine solution was used to trap the possible traces of ionic and organic Hg(II) purged out from the reaction unit due to N_2 gas flow. Hg(0) was eventually captured in an acidic $KMnO_4$ solution in the form of Hg(II). Each 5 ml trap solution was collected at the given time intervals. After a reduction of excess $KMnO_4$ by titration with 20% (w/v) hydroxylamine hydrochloride solution until the red-purple color totally disappeared, the total Hg in the trap solution was measured by cold vapor atomic absorption

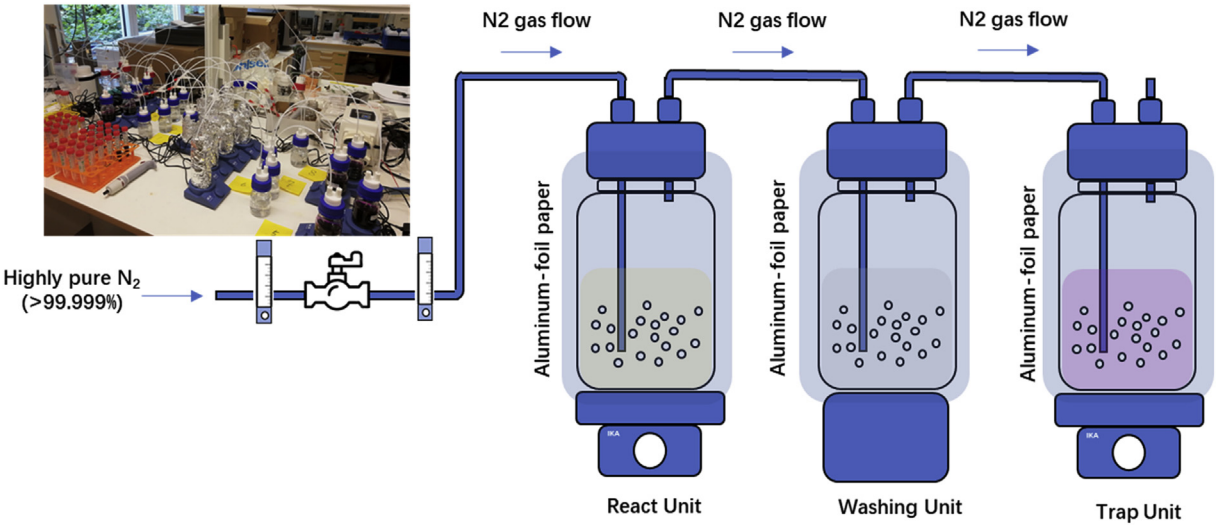

Fig. 2. Illustration of the abiotic dark reduction experimental setup and photograph of the working system. Reaction unit (100 mL) containing DOM with added Hg(II) (total of 50 mL) covered with aluminum foil papers to avoid light irradiation; Washing unit containing 0.1% (w/v) cysteine solution (60 mL); Trap unit containing 85 mL $KMnO_4$ solution prepared with 0.2% (w/v) $KMnO_4$ in 4% (v/v) H_2SO_4. Units are linked by Teflon® tubes. The experimental temperature was 25 ± 3 °C.

spectrometry (CVAAS) (CA-205, Shanghai Jingmi Instrument, China) (Jiang et al., 2014, 2015). For each experimental condition, duplicates were conducted for each DOM sample. Two control experiments, including DOM alone and Hg(II) alone, were prepared as blanks for all of the experiments. Blank values were used to correct the Hg(0) production by subtraction to remove the backgrounds. Hg(0) produced by reduction was shown as the percentage (%) of initial Hg(II) added into the reaction unit. Due to no organic interference in the trap unit, the total Hg(0) trapped by $KMnO_4$ after decolorization by $NH_2OH{\cdot}HCl$ was directly reduced with $SnCl_2$, and then, the Hg(II) quantity was measured by CVAAS (USEPA Method 245.1). The detection limit of the mercury analysis instrument is 3 ng $.L^{-1}$.

2.3.2. ARC_{Hg} calculation and kinetic fitting

According to the terminology of reducing capacity in Peretyazhko and Sposito (2006), the ARC_{Hg} is a specific reducing capacity parameter representing the native reducing capacity of DOM without pre-reduction and other manipulations, which is directly derived from Hg(II) reduction instead of Fe(III) or other oxidants. As 1 mol Hg(II) needs 2 mol of electrons to form Hg(0), the ARC_{Hg} values of all samples were calculated by the electrons transferred per unit amount of DOC at the kinetic end (i.e., 72 h). With regards to kinetics, Hg(II) reduction entered into a slow phase and reached a plateau after 24 h. Thus, 72 h is sufficient as the endpoint.

In this study, we thus assumed a pseudo-first-order rate law for fitting the kinetic process for simplicity by accounting for one or two redox-active pools of DOM (Bauer et al., 2007; Pham et al., 2012). The two pools are defined as DOM_1, the kinetically labile electron donating components (e.g., hydroquinones, and other polyphenolic moieties), and DOM_2, the less labile electron donating components (e.g., nonquinone moieties), respectively:

$$d([Hg^0]/[Hg(II)]_0)/dt = -k_{obs\ 1} \times ([DOM]_1/[DOM]_{bulk\ DOC}) - k_{obs\ 2} \times ([DOM]_2/[DOM]_{bulk\ DOC}) \quad (7)$$

The time-dependent solution to Eq (7) leads to Eq (8):

$$([Hg^0]/[Hg(II)]_0)(t) = DOM_1 \times (1-e^{-kobs1 \times t}) + DOM_2 \times (1-e^{-kobs2 \times t}) \quad (8)$$

where $[Hg^0](t)$ is the concentration of the reduction product formed (Hg(0)) at the time point of the kinetic process, $k_{obs\ 1}$ and $k_{obs\ 2}$ represent the two kinetic phases including the rapid and slow stages, respectively; and DOM_1 and DOM_2 are the proportions of bulk DOM representing the two different DOM pools, respectively. The two DOM pools are constrained by $DOM_1 + DOM_2 \leq 100\%$. $[Hg(II)]_0$ is the initial Hg(II) concentration in react system.

2.3.3. Quality assessment and control

A pure-procedure for heavy metal analysis was conducted in this study. The detection limit of this reduction system (i.e., method detection limit) was 15 ng. L^{-1} (Hg(II)). All results were reported as the mean values ± standard deviation, and statistical analyses were performed in OriginPro® 2017 and SPSS® 24. The detailed descriptions of quality assessment and control are listed in the Supporting Information.

3. Results and discussion

3.1. DOM properties and origins

3.1.1. DOC and CDOM

The DOC concentration ranged from 1.17 to 33.81 mg. L^{-1} with obvious spatial variation (coefficient of variation (CV) = 90%). The three regions were significantly different from each other ($p = 0.015$). Mountain lakes were generally clear water lakes with the lowest DOC (3.32 ± 1.71 mg. L^{-1}), whereas the southern boreal forest lakes were the most colored (CDOM 46.59 ± 19.37 m^{-1}) with the highest DOC concentration of 17.40 ± 6.83 mg. L^{-1} (Fig. 3a). After normalizing the CDOM by the DOC, the CDOM/DOC ratio was used for estimating the relative proportion of chromophores in bulk DOC. Among the three regions, the average CDOM/DOC values were 1.93 ± 0.64 (tundra lakes), 1.08 ± 0.42 (mountain lakes), and 2.67 ± 0.39 (boreal forest lakes), respectively. This was indicative of the relative contribution of CDOM to the bulk DOC, which was greatest in the lakes influenced by forests. The high coefficient of determination ($r^2 = 0.95$) of CDOM versus DOC for all samples (Fig. 3b) indicates that variations of chromophores in waters are a key factor in the DOC spatial variations.

Previous studies have revealed that the surrounding landscape (i.e., land cover types) and climate control the quality and

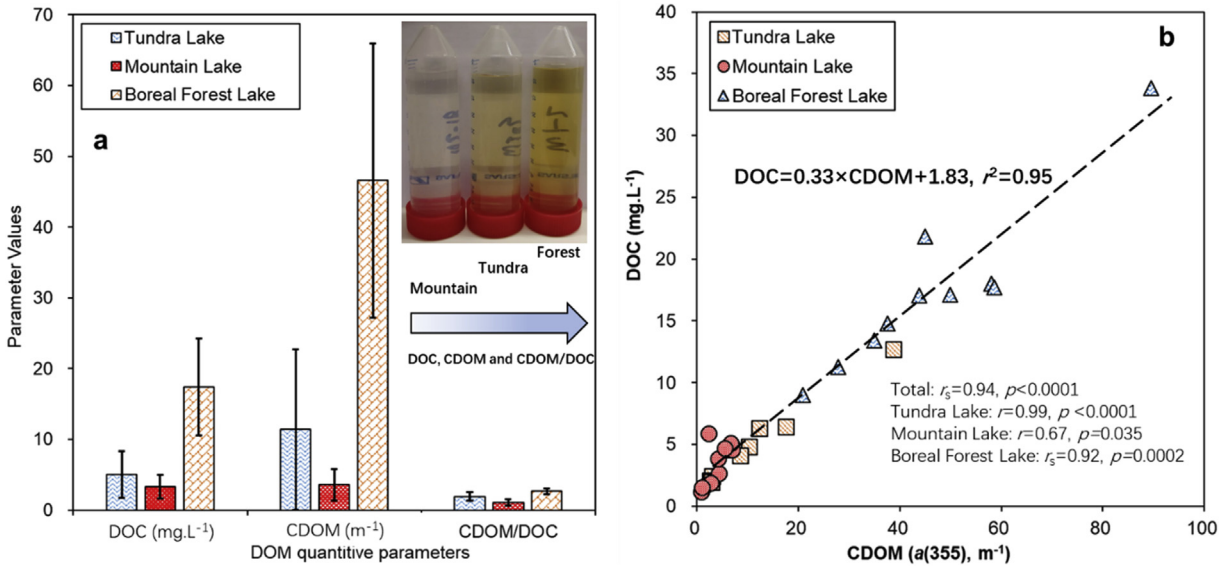

Fig. 3. Differences in the DOC and CDOM: (a) comparisons of the three categories of lakes (inserted photo shows the typical watercolor from the three types of lakes) and (b) relationships between the DOC and CDOM. The dashed line in the plot (b) shows the linear regression fitting.

quantities of DOM in northern lakes (Kothawala et al., 2014; Larson et al., 2014) including high-latitude lakes (Osburn et al., 2017). Kellerman et al. (2014) suggested that lakes with high DOC concentrations contain the most diversity of DOM because of new terrestrial imports. Thus, it was not surprising to observe the highest DOC and CDOM in boreal forest lakes in this study. In contrast, the mountain lakes showed the lowest CDOM and DOC, which can be attributed to the colder climate, less precipitation, and lack of vascular plant coverage, which resulted in less terrestrial DOM inputs compared to tundra and boreal areas. For tundra lakes in Norway, located more than 300 km northwest of the mountain lakes, the rich humic tundra soils provide more terrestrial DOM input due to the frozen soil thawing and increasing precipitation in the summer, which explains the higher DOM than mountain lakes but less than forest lakes.

3.1.2. DOM optical properties and origins

The DOM optical properties were obviously different among the three groups of lakes (Fig. 4). An higher $SUVA_{254}$ after iron correction implies higher DOM aromaticity, indicating the greater contributions of allochthonous inputs of DOM (Weishaar et al., 2003). As shown in Fig. 4a, the highest values were observed in boreal forest lakes (4.00 ± 0.40 L. mg $C^{-1}.m^{-1}$). However, in Arctic lakes, DOM from tundra lakes (3.05 ± 0.76 L. mg $C^{-1}.m^{-1}$) showed higher aromaticity than that from mountain lakes (2.11 ± 0.53 L. mg $C^{-1}.m^{-1}$). In contrast to the study by Ripszam et al. (2015), we did not observe a decline in the aromaticity of DOM from high to low latitudes. Additionally, the S_R usually is negatively correlated with the DOM molecular mass (Helms et al., 2008; Fichot and Benner, 2012; Fichot et al., 2013). The greatest S_R value (1.00 ± 0.16) was found in mountain lakes, followed by tundra lakes (0.86 ± 0.09) and forest lakes (0.73 ± 0.02), which reflected that the DOM with higher aromaticity and molecular mass in lakes was greatly influenced by forests, rather than tundra, bushes, lichens, or mosses, which was further validated by the fluorescence parameters. The FI (1.35 ± 0.06) and BIX (0.63 ± 0.03) values of boreal forest lakes were close to the allochthonous end-member (FI = 1.4, BIX = 0.7) (McKnight et al., 2001; Huguet et al., 2009), and mountain lakes (FI, 1.67 ± 0.31; BIX, 0.89 ± 0.16) were more adjacent to the autochthonous end-member (Fig. 4b and c). Additionally, a higher RFE indicates a higher relative amount of algal compared to non-algal inputs (Downing et al., 2009; Hansen et al., 2016). The distribution of the RFE displays the highest values in Arctic lakes and lowest in boreal forest lakes (Fig. 5b).

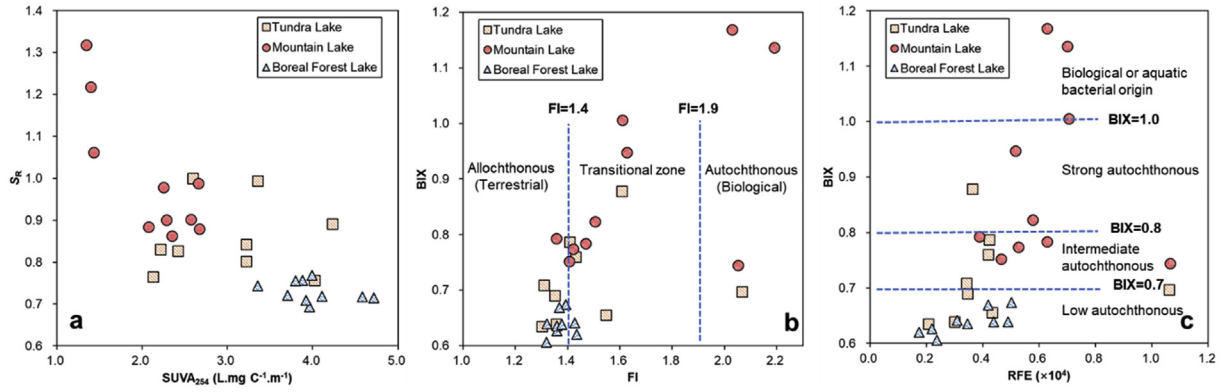

Fig. 4. Comparison plots of the (a) $SUVA_{254}$ versus S_R, (b) FI versus BIX, and (c) RFE versus BIX values for all DOM samples.

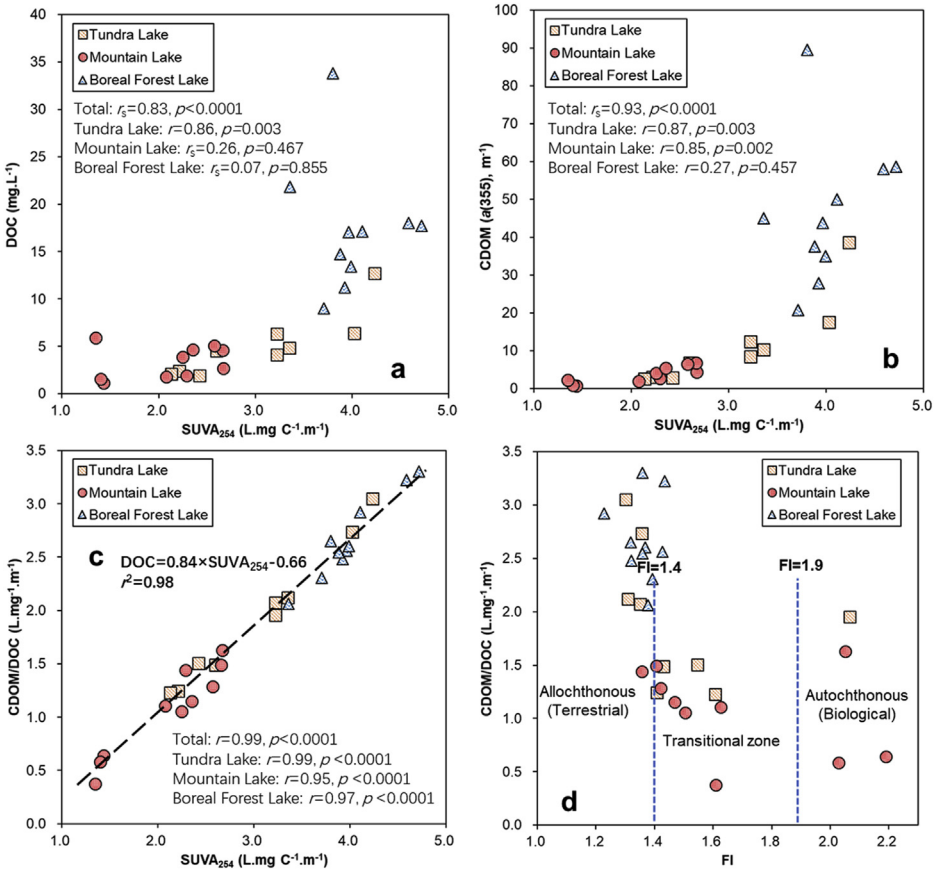

Fig. 5. Comparison plots of the (a) SUVA$_{254}$ versus DOC, (b) SUVA$_{254}$ versus CDOM, (c) SUVA$_{254}$ versus CDOM/DOC, and (d) FI versus CDOM/DOC values for all DOM samples.

In terms of aromaticity, poor explanations for DOC variations were observed in the mountain and forest lakes (Fig. 5a) as well as for the CDOM only in forest lakes (Fig. 5b) due to the limited size of the dataset. However, aromaticity showed a highly significant correlation with the DOC and CDOM, respectively, for all datasets for all three regions (Fig. 5a–b). This suggests that DOC and CDOM are still relevant to reflect the changes in DOM aromaticity in overall areas and could be used to estimate the variation of DOM aromaticity in less-equipped conditions for DOM characterization. Meanwhile, the ratio of CDOM/DOC showed a highly significant correlation with the SUVA$_{254}$ in the three categories of lakes (Fig. 5c) and can be strongly explained by the aromatic difference ($r^2 = 0.98$). The relatively higher proportion of CDOM, which reflects the obvious terrestrial characteristics (Fig. 5d), as similar to Fig. 5b, supports this. However, it should be emphasized that the good correlation between SUVA$_{254}$ and the DOC concentration may lead to a problem that it might not accurately estimate the biogeochemical reactivities of DOM by only focusing on the DOM characteristics if the reactions are also influenced by DOC concentrations (e.g., reactant/DOC ratios) (see 3.2. Ambient reducing capacity determination and kinetic fitting).

3.1.3. N/C ratios and the two end-member mixing model

In addition to optical indicators (e.g., FI), we used the N/C molar ratios and the classic model of two end-member mixing to estimate the relative contributions from allochthonous and autochthonous sources to the bulk DOM. A simple comparison of N/C molar ratios within well-characterized reference samples from the International Humic Substances Society (IHSS) (Fig. 6a) showed that DOM in this study is from multiple sources. Higher N/C ratios from Arctic lakes (VIII and IX regions in Fig. 6a) were similar with fulvic acid and bulk soils samples, which were higher than the average N/C ratio (0.038 ± 0.021). In contrast to the Arctic lakes, boreal forest lakes showed closer value ranges (0.015–0.026) to reference bulk NOM collected from terrestrial-influencing aquatic systems (0.018-0.021) such as the Suwannee River within a significant proportion of allochthonous OM. Meanwhile, the f_{auto} was the highest in mountain lakes ($50 \pm 15\%$) followed by tundra lakes ($27 \pm 10\%$), as shown in the two end-member mixing model (Fig. 6b). However, samples from forest lakes ($89 \pm 3\%$) showed predominant allochthonous contributions. Thus, our results further demonstrate that the DOM in Arctic lakes is less terrestrial-dominant than in reference sites (i.e., forest lakes). Between the two categories of Arctic lakes, tundra lakes are more terrestrial-influenced compared to mountain lakes.

3.2. Ambient reducing capacity determination and kinetic fitting

3.2.1. Experiment 1: same Hg addition

With the same Hg addition, the ambient reducing capacities of DOM were determined by reacting ~286 nM Hg(II) with original DOM samples with a large DOC concentration range (1.17–33.81 mg C.L^{-1}) for 72 h continuous purging kinetic experiments under dark anoxic conditions. The Hg/DOC ratios varied within the range of 5.2–14.9 mg .g^{-1}, with the boreal lake DOM showing the lowest Hg/DOC ratios due to the highest DOC concentrations (9.02–33.81 mg C.L^{-1}). Among all of the samples, the ARC$_{Hg}$ ranged from 0.17–5.61 mmol e$^-$·mol C^{-1} (mean 2.17 ± 1.78 mmol e$^-$.mol C^{-1}), which were significantly different among the three categories (Fig. 7a). Mountain lake DOM showed

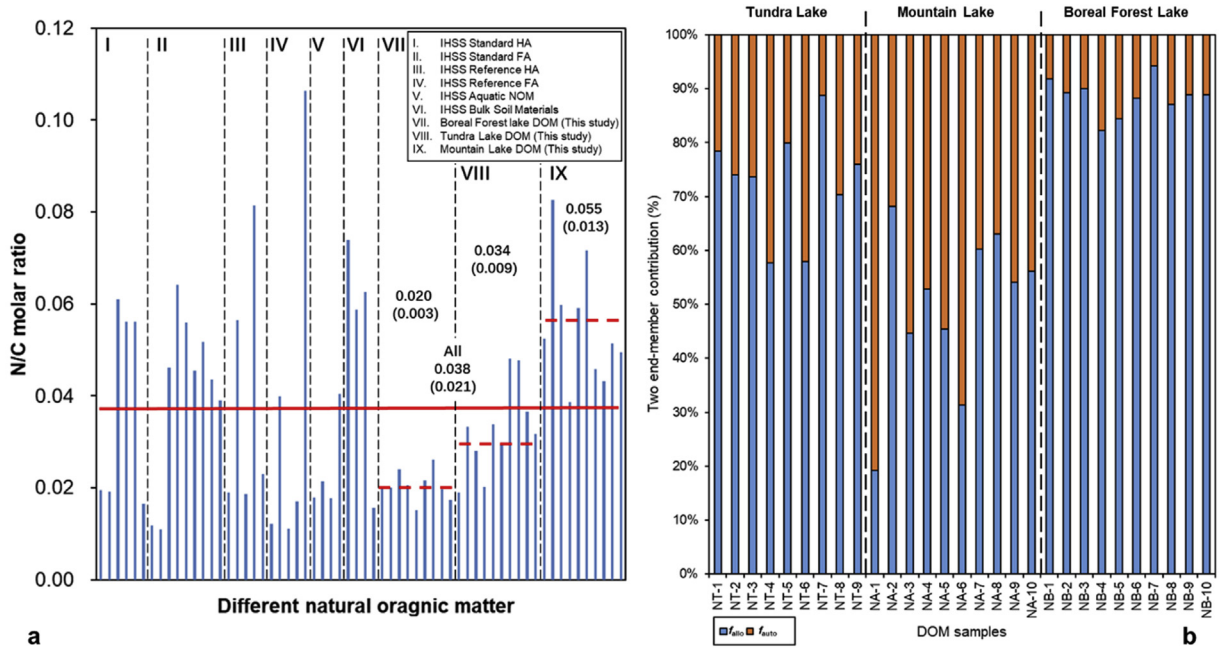

Fig. 6. N/C molar ratios of different natural organic matter and the two end-member mixing model. In plot (a), the elemental compositions of reference materials were collected from the IHSS website (http://humic-substances.org/elemental-compositions-and-stable-isotopic-ratios-of-ihss-samples/). VII, VIII, and IX regions were samples from the boreal forest, tundra, and mountain lakes in this study, respectively. Values (i.e., average values (sd)) indicate the average N/C molar ratio for samples delimited by different lengths of the red line. In plot (b), orange and blue colors represent allochthonous (f_{allo}) and autochthonous (f_{auto}) fractions, respectively. (For interpretation of the references to color in this figure legend, the reader is referred to the Web version of this article.)

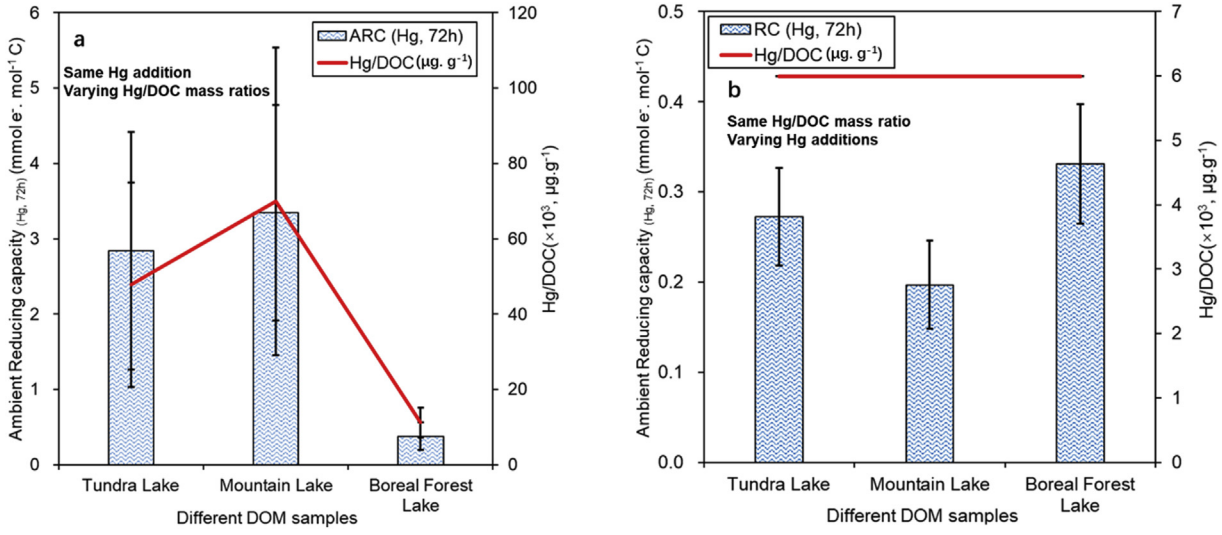

Fig. 7. Calculated ambient reducing capacity values (ARC_{Hg}) and the corresponding various Hg/DOC mass ratios ($\mu g.g^{-1}$) at 72 h under two experimental conditions including (a) same Hg(II) addition but various Hg/DOC mass ratios ($\mu g.g^{-1}$) and (b) same Hg/DOC mass ratio ($\mu g.g^{-1}$) but various Hg(II) additions.

the highest value (3.34 ± 1.43 mmol e^-.mol C^{-1}), while boreal lake DOM had the lowest (0.38 ± 0.185 mmol e^-.mol C^{-1}).

As shown in Table 1, correlation analysis showed the quantitative and characteristic parameters of DOM including the $SUVA_{254}$, CDOM, CDOM/DOM, DOC, and f_{allo}; all of them showed significant negative correlations with the ARC_{Hg}. In contrast, the ARC_{Hg} was positively correlated with the RFE, S_R, FI, $f_{auto,}$ and BIX. In appearance, these correlations might lead to a conclusion that the DOM with higher terrestrial contributions (i.e., boreal lake DOM) had a lower reducing capacity compared to the higher electron donations from autochthonous-derived DOM (i.e., mountain lake DOM), which is different from our initial expectation that autochthonous-dominant DOM has a lower RC values because of less aromaticity.

However, it should be emphasized that the large variations of Hg/DOC ratios should be considered to understand the relationship between the reducing capacity of DOM and its characteristics. Previous studies have reported that the relative proportion of electron acceptors (e.g., Fe(III)/DOC or Hg(II)/DOC ratio) has a predominant influence on the observed reducing capacity of DOM (Bauer et al., 2007; Zheng et al., 2012; Jiang et al., 2014, 2015). In this study, the DOC showed highly positive correlations with these characteristic parameters of DOM (e.g., $SUVA_{254}$ (Fig. 5a), CDOM

Table 1
Correlation analysis of the ambient reducing capacity (ARC_{Hg}) with other quantitative and qualitative parameters at two experimental conditions.

		$SUVA_{254}$	S_R	FI	BIX	RFE	f_{allo}	f_{auto}	DOC	Hg/DOC	CDOM	CDOM/DOC
Exp#1, Same Hg addition: (1) Varying DOC; (2) Varying Hg/DOC mass ratio												
ARC_{Hg} ($n = 29$)[b]	Correlation coefficient	−0.70 (r)[a]	0.50 (r)	0.40 (r_s)	0.71 (r_s)	0.39 (r)	−0.68 (r)	0.68 (r)	−0.91 (r_s)	0.91 (r_s)	−0.82 (r_s)	−0.66 (r)
	p value	<0.001	0.006	0.033	<0.001	0.036	<0.001	<0.001	<0.001	<0.001	<0.001	<0.001
Exp#2, Same Hg/DOM mass ratio: (1) Varying DOC; (2) Varying Hg additions												
ARC_{Hg} ($n = 29$)	Correlation coefficient	0.69 (r)	−0.50 (r)	−0.65 (r_s)	−0.70 (r_s)	−0.56 (r)	0.66 (r)	−0.66 (r)	0.64 (r_s)	/[c]	0.72 (r_s)	0.69 (r)
	p value	<0.001	0.005	<0.001	<0.001	0.002	<0.001	<0.001	<0.001	/	<0.001	<0.001

[a] According to the dataset normal distribution or not, r and r_s in brackets denote Pearson's and Spearman's rank correlation coefficients, respectively.
[b] Total number of DOM samples ($n = 29$) from the three categories of lakes.
[c] The symbol of "/" denotes that this parameter was not accounted for.

(Fig. 3b), N/C and f_{allo} (Table S1, Supporting Information)), and negative correlations with the RFE, f_{auto}, FI and BIX (Table S1, Supporting Information), indicating that high DOC concentrations, for example in boreal lakes, are associated with high terrestrial inputs. As a result, the lowest ARC_{Hg} value was observed in boreal lake DOM with the same Hg addition amount in the experiment, which reflects the relative deficiency of electron acceptors (i.e., Hg(II)) rather than the relative insufficient electron donation capacities. The results of this experiment explain why the reducing capacity of DOM is not easy to be observed in the situation of an overly high DOC concentration (e.g., 50 mg $.L^{-1}$) (Zheng et al., 2012; Jiang et al., 2014, 2018b), even though the DOM is highly terrestrial-dominant.

Furthermore, to avoid the multicollinearity between the quantitative (e.g., Hg/DOC and DOC) and qualitative parameters (e.g., $SUVA_{254}$) of DOM, we used partial least squares (PLS) regression to fit and track the relative contributions of different influencing factors (e.g., DOC, Hg/DOC ratios, $SUVA_{254}$ and FI) to the ARC_{Hg} (Fig. S1, Supporting Information). The results support that the Hg/DOC ratios resulting from DOC variations together explained 85% of relative variance contributions for ARC_{Hg} variations, in contrast to the contributions from DOM properties including its origins.

3.2.2. Experiment 2: same Hg/DOC ratios

Under the condition with the same Hg/DOC ratio (6 mg.g^{-1}), the ARC_{Hg} differences among the three groups followed the order of boreal forest lakes (0.33 ± 0.07 mmol e^-.mol C^{-1}), tundra lakes (0.27 ± 0.05 mmol e^-.mol C^{-1}), and mountain lakes (0.20 ± 0.05 mmol e^-.mol C^{-1}) (Fig. 7b). As the proportion of Hg relative to the specific electron pool of individual DOM is identical, the Hg/DOC ratio could not be an influencing factor, and the differences in the ARC_{Hg} can only be explained by the differences in the electron donation capacities of DOM. The ARC_{Hg} values of all samples decreased with increasing autochthonousness of the DOM (Table 1). The ARC_{Hg} showed significant negative correlations with the FI, f_{auto}, S_R, BIX and RFE and positive correlations with the $SUVA_{254}$, DOC, f_{allo}, CDOM, and CDOM/DOM. These correlations suggest that DOM with a greater terrestrial contribution has a higher electron donation capacity. The higher aromaticity and molecular size of aquatic DOM might enrich the redox-reactive functional groups such as polyphenols and quinones, thus resulting in greater electron shuttle capacities for diverse aquatic DOM samples (Scott et al., 1998; Aeschbacher et al., 2012; Sharpless et al., 2014).

Aeschbacher et al. (2012) quantified the electron donation capacities of different aquatic NOM samples from lower latitudes by mediated electrochemical oxidation methods. They found that NOM from a sphagnum bog (mainly terrestrial plant inputs) and a coastal pond in Antarctica (mainly lichen and microorganism inputs) could be the typical two end-members and showed the highest and lowest reducing capacities, respectively, compared to the NOM of mixed origins, such as Suwannee River with NOM in the middle (Aeschbacher et al., 2012). Thus, the effects of the aquatic DOM origins on the ARC reflect the vital role of phenolic and quinone moieties derived from terrestrial higher plants. Our study agrees with their findings, showing a similar order of the RC values based on the influence of terrestrial inputs: boreal forest lakes (high) > tundra lakes (median) > mountain lakes (low) (Table 1 and Fig. S2, Supporting Information)

Additionally, after comparing the ARC_{Hg} values from the two experiments (Exp# 1 and Exp# 2), the observed changes in the ARC_{Hg} observed were not proportional to the changes of Hg/DOC by the same ratio (Fig. S3, Supporting Information), which further implies the importance of heterogeneous DOM structures. Steric extension of the DOM structure might affect the availability of electron donating moieties. This may be the reason for the linear deviations (i.e., non-linear change) of the electron transfer capacity, while the Hg/DOC decreased, which was caused by increasing the DOC beyond a certain threshold concentration (Gu and Chen, 2003; Blodau et al., 2009; Zheng et al., 2012; Jiang et al., 2014). Thus, the calculated reducing capacity from manipulating bulk DOM, especially the dilution of higher DOC concentrations into lower ones, may overestimate the ambient reducing capacities of DOM when its concentration (i.e., DOC) is high in a real environment.

3.2.3. Kinetic fitting

Hg species are involved in binding with weak (e.g., RO/N containing groups) and strong (e.g., RSH groups) sites of NOM and are a crucial factor to control the complete kinetics and thermodynamics (Jiang et al., 2015; Zheng et al., 2012; Gu et al., 2011). We estimated the concentration of RSH to be 0.15% of the DOC mass (Skyllberg, 2008; Jiang et al., 2015) or 0.5 μM RSH at 10 mg L^{-1} DOC; thus, the threshold of the Hg/DOC mass ratio accounting for Hg saturation with strong sites of RSH, such as in the form of $Hg(SR)_2$, is approximately 4.6 mg.g^{-1}. This threshold is less than the lowest Hg/DOC (5.2 mg.g^{-1}) of samples, suggesting the oversaturation of Hg with RSH in this study. Thus, Hg species with O/N containing groups (i.e., $Hg(OR)_2$ and RSHgOR) are the predominant species. Hence, the influence of competition for Hg binding between weak and strong reduction sites is unlikely to be a limiting factor to control the complete kinetics in this study. Instead, kinetics are mainly dependent on the electron donations from DOM.

Previous works have identified two redox-reactive functional groups participating in the electron transfers of NOM, but only one is related to quinone moieties (Ratasuk and Nanny, 2007; Pham et al., 2012; Hernández-Montoya et al., 2012), which controls the rapid and slow kinetic phases. Based on the average kinetic curves of the three categories of DOM (Fig. 8), the fitted kinetic results were obtained by Eq (5) and are listed in Table 2. The ranges of k_{obv1} and k_{obv2} were 0.10–0.19 h^{-1} and 0.001–0.004 h^{-1}, respectively. The kinetic rates controlled by the labile electron donation component of DOM (DOM_1) were greater than by the less labile

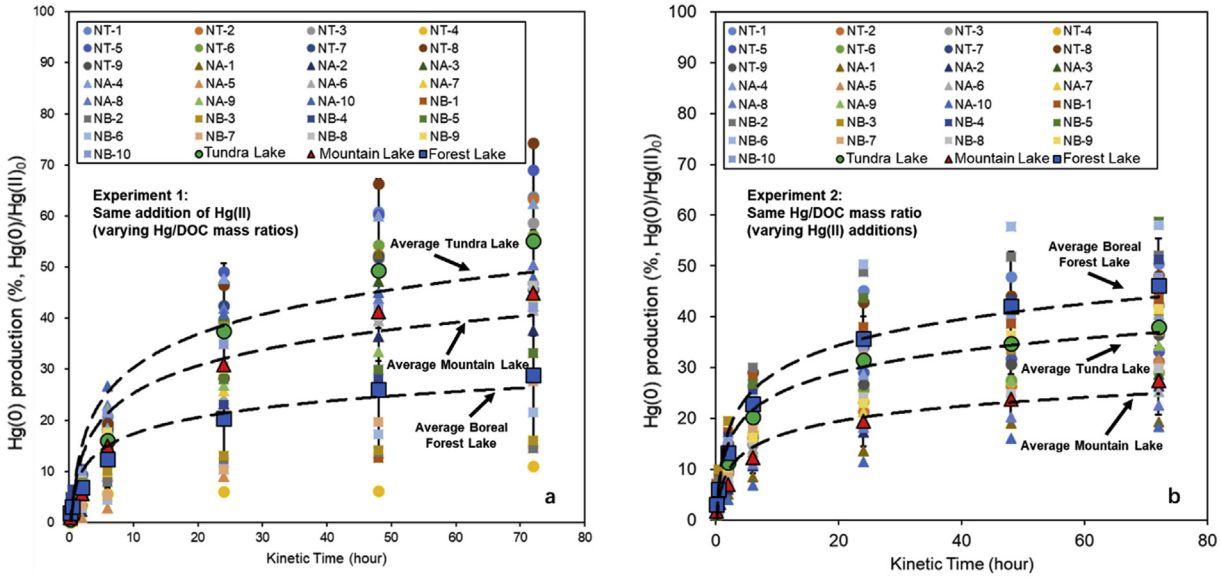

Fig. 8. Abiotic, dark reduction kinetics of Hg(II) by different DOM samples in two experimental conditions including (a) Exp #1, same Hg(II) addition but various Hg/DOC mass ratios ($\mu g \cdot g^{-1}$) and (b) Exp #2, same Hg/DOC mass ratios ($\mu g \cdot g^{-1}$) but various Hg(II) additions. In the legends, NT, NA and NB represent the samples from tundra, mountain and boreal forest lakes, respectively. Black dashed lines represent the fitting curves of the average kinetics of three types of DOM samples by the pseudo-first-order rate law, respectively.

Table 2
Kinetic fitting results by the pseudo-first-order rate law regarding the two DOM pools.

Experimental Conditions	DOM samples	DOM_1	k_{obv1} (h^{-1})	DOM_2	k_{obv2} (h^{-1})	r^2
Exp#1, Same Hg addition:	Tundra Lakes	0.26	0.13	0.73	0.003	0.85
(1) Varying DOC	Mountain Lakes	0.31	0.10	0.69	0.002	0.98
(2) Varying Hg/DOC mass ratio	Boreal Forest Lakes	0.10	0.19	0.89	0.004	0.94
Exp#2, Same Hg/DOM mass ratio:	Tundra Lakes	0.27	0.14	0.69	0.001	0.90
(1) Varying DOC	Mountain Lakes	0.16	0.11	0.82	0.002	0.94
(2) Varying Hg additions	Boreal Forest Lakes	0.31	0.18	0.69	0.004	0.98

part (DOM_2). DOM_1 and DOM2 contributed 10–31% and 69–89% to the overall electron donations, respectively. The proportions of the two DOM pools were similar to Bauer et al. (2007), who used the iron-test method and reported fractions of 20–44% (DOM_1) and 56–80% (DOM_2) for the rapid and slow phase, respectively. Additionally, in some cases, the sum of DOM_1 and DOM_2 is less than 100% (Table 2), suggesting that a small fraction (1–4%) of redox moieties of DOM were inert and did not participate in the reaction.

For each category of DOM samples, the k_{obv} values for the two kinetic phases were similar (Table 2) between the two experimental conditions, indicating that the kinetics of electron transfers from the two DOM pools are independent of the Hg/DOC ratio but associated with its intrinsic reducing capacity. In contrast, the fraction changes of the two DOM pools at the two different experimental conditions suggest the inconsistent relative proportions of labile and less labile electron donation components in DOM, which may change due to the Hg/DOC variations. Thus in Exp# 1, for the mountain lake DOM, the greatest DOM_1 (31%) is attributed to the highest Hg/DOC resulting in the highest observed ARC_{Hg} values, even though the k_{obv} is the slowest ($k_{obv1} = 0.10\ h^{-1}$ and $k_{obv2} = 0.002\ h^{-1}$ on average) compared to the DOM from tundra ($k_{obv1} = 0.13\ h^{-1}$ and $k_{obv2} = 0.003\ h^{-1}$ on average) and forest lakes ($k_{obv1} = 0.19\ h^{-1}$ and $k_{obv2} = 0.004\ h^{-1}$ on average). Since rapid reduction is the key step for Hg(II) reduction, k_{obv1} decreased in the sequence of boreal forest lakes > tundra lakes > mountain lakes, which further supports that the highest reducing capacity was in boreal forest lakes, rather than the mountain lakes, which was misled by the interference of various Hg/DOC mass ratios.

3.3. Influence of complexed iron(II)/iron(III) and pH

Previous studies have suggested that the influence of complexed iron could be a potential source of the reducing capacity from NOM (Struyk and Sposito, 2001; Peretyazhko and Sposito, 2006). Purification for removing the iron is not practical if we consider that the bulk DOM is also a system within predominant organic components under ambient inorganic conditions (Kothawala et al., 2014). However, the electron contribution from complexed Fe(III)/Fe(II) would require a very high prior loading of iron for low carbon/iron molar ratios (e.g., 2–7 (Xie and Shang, 2005)) in order to be significantly observed (Struyk and Sposito, 2001; Xie and Shang, 2005). In this study, all DOM samples contain iron within a narrow range of 0.11–0.46 $mg.L^{-1}$, which is $0.16 \pm 0.05\ mg.L^{-1}$ in tundra lakes, $0.13 \pm 0.01\ mg.L^{-1}$ in mountain lakes, and $0.21 \pm 0.09\ mg.L^{-1}$ in forest lakes, respectively. Therefore, the carbon/iron molar ratios were in the range of 33–723 (average 232 ± 183), in which the Fe content in DOM samples was far less than carbon by at least two orders of magnitude. Meanwhile, a simple estimation of an extreme situation assuming that all iron is Fe(II) and can donate electrons by a 1:1 M stoichiometry, showed that the calculated contributions to reducing capacities from Fe(II) were only accountable for only 0.1%–3.0% of the observed ambient reducing capacities of DOM. Additionally, the redox buffering mechanism of DOM for preserving Fe(II) (Daugherty et al., 2017) could inhibit the influence of iron on the redox properties of DOM itself in such narrow kinetic window (i.e., 72 h). As a consequence, iron in DOM is unlikely to substantially affect the reducing capacity

observed.

On the other hand, the influences of pH on the redox characteristics of DOM mainly include (1) speciation of the chemical probe (e.g., heavy metals) and (2) DOM steric structures. Both indicate that the reduction of Hg by various DOM could be strongly pH-dependent. Previous studies have shown that the pH influence on the NOM redox characteristics involves deprotonation and protonation, which resulted in effects of either enhancement or inhibition (Helburn and MacCarthy, 1994; Bauer et al., 2007; Ratasuk and Nanny, 2007; Aeschbacher et al., 2012; Jiang et al., 2014; Walpen et al., 2018). However, the pH of all DOM samples showed a narrow range of 4.64−5.77 in this study, compared to the above literature that had large pH differences. Furthermore, no significant correlation was found between the pH and the ARC_{Hg} at two conditions (Fig. S4, Supporting Information), which may excludes the possibility of a substantial effect from pH changes.

3.4. Notes and limits

Several previous studies have illustrated that quinone moieties, as the most redox-prone component of natural organic matter, could be derived from the degradation of lignin (i.e., terrestrial inputs) and microbial synthesis (i.e., internal aquatic processes) (Stevenson, 1994). McKnight et al. (1991) extracted fulvic acid from Lake Fryxell of the Antarctic, which, despite being devoid of vascular plants, showed obvious redox properties (Scott et al., 1998). The similar redox characteristic was also observed in sample from Pony lake of the Antarctic (Aeschbacher et al., 2012). Thus, besides the terrestrial-dominant DOM pool, even DOM from the aquatic environments influenced less by terrestrial inputs, such as the reported Antarctic lakes and the Arctic lakes in this study, can still serve as electron donors. Additionally, all DOM samples in this study were not pre-reduced and kept their original status without manipulation. The observed reducing capacities substantiate that some portion of the redox components (e.g., phenolic and semiquinone moieties) cannot be fully oxidized and reserve the potential for electron donation to certain degrees even in air-exposure conditions. This is supported by the previous works (Ratasuk and Nanny, 2007; Bauer and Kappler, 2009) and the study even including the fully reoxidized DOM samples (Maurer et al., 2010).

Additionally, it should be emphasized that we cannot extend too much of the influences of the DOM reducing capacity to Hg geochemistry, as the higher Hg/DOC mass ratios used in this study were higher than ratios in the pristine environment (less than ~0.1 mg $.g^{-1}$). However, this study used the Hg reduction process to assess the electron donation potential of DOM, which might partially unveil the effect of DOM on Hg abiotic reduction in highly contaminated aquatic sites, such as the rice paddy fields and lakes in Hg mine areas (Zhao et al., 2016; Feng et al., 2018). This study revealed that the ARC_{Hg} values are not only controlled by the DOM composition and origins but also related to the complexation with DOM involving metals/DOC ratios. On the other hand, from the perspective of the Hg biogeochemical cycle and atmosphere-surface exchange (Zhu et al., 2016), our results could further provide a partial explanation to estimate whether organic-rich environments are sinks (Osterwalder et al., 2017) or sources (Jiskra et al., 2015; Zhu et al., 2018) for the mercury cycle, particularly in the Arctic regions, which have been estimated as globally significant mercury (Schuster et al., 2018) and terrestrial organic carbon pools (Vonk et al., 2015). Without regards to the deficiency of electron acceptors (e.g., Hg(II)), only focusing on the electron donation pool, as shown in Exp# 1, could lead to the misjudging of the reducing capacities of DOM in real situations. Furthermore, the results from this study show that the DOM origins and composition have a large impact on its reactivity with Hg, which supports our previous observation (Jiang et al., 2018a, b) and other reports (Schartup et al., 2015b; Jonsson et al., 2017). Importantly, this study further illustrates that DOM optical characterization is a useful tool for unveiling the relationship between DOM and Hg (Lescord et al., 2018).

However, the limitations of this study need to be noted. The experiments were conducted in constant room temperature and cannot represent the actual temperature variation in the real environment, which may be particularly critical for investigating the changes in DOM in the Arctic lakes that are experiencing global warming. Additionally, competition from other divalent cations, higher iron/carbon ratios in some environments, and the influences of pH and high concentrations of chloride are still unknown. Additionally, this study is specifically designed to investigate the spatial variations of DOM associated with the ambient reducing capacity, instead of on a temporal scale. Hence, further temporal long-term investigation and repetitions will be necessary on laboratory-scale and natural aquatic systems, respectively.

4. Conclusion

Our study examined the influences of the DOM origins and properties on its ambient reducing capacity in high-latitude lakes. The results demonstrated that DOM, as an electron provider, is ubiquitous in aquatic systems regardless of latitudes. The effects of the DOM origins on the reducing capacities reflect that terrestrial-dominant DOM (e.g., in boreal forest lakes) is more reactive than DOM with a reduced terrestrial property (e.g., Arctic including tundra and mountain lakes). However, only the DOM quality cannot explain the observed differences in the ARC. This study highlights that terrestrial-dominant characteristics of DOM with higher aromaticity could not ensure a significantly greater electron donation in practical observations. As a relative indicator, the ARC is also dependent on the relative proportions of oxidants and the DOM concentration (i.e., DOC), for example, the Hg/DOC ratio in this study. Therefore, when using heavy metals as oxidants for measuring the reducing capacity, we suggest that comparisons among different DOM samples can be conducted while the oxidant/DOC ratios are kept the same level and should be reported.

On the other hand, regarding DOM being a black box mixture, it is recommended to use the ARC without manipulation to reflect the native electron transfer capacity of DOM in the given environmental conditions, which is also more relevant to real circumstances. Additionally, as a supplement for the traditional chemical probe methods for reducing capacity measurements, the Hg(II) reduction method can be used even in high DOC conditions, especially organic-rich environments, such as humic lakes or eutrophic waters. As projected in the Arctic region, permafrost thaws heavily influence the composition and characteristics of DOM in Arctic aquatic systems, which imposes further feedback on the carbon cycle and thus climate change. Consequently, further investigation of the coupling influences of DOM on mercury and carbon cycles in the future may establish links between Hg cycles in the context of climate change, especially in the rapidly changing Arctic regions.

Declaration of competing interest

The authors declare that they have no known competing financial interests or personal relationships that could have appeared to influence the work reported in this paper.

Acknowledgments

This research was financially supported by National Science

Foundation of China (41977275, 41403079) and Internal Funding for Early Careers from the Department of Forest Ecology and Management (FEM) of Swedish University of Agricultural Science (SLU) and Swedish Infrastructure for Ecosystem Science (SITES). Dr. Tao Jiang personally gives his appreciation to funding provided by the Sino-Swedish Mercury Management Research Framework (SMaRef) of Swedish Research Council (VR) (No.D697801), for generously supporting his researcher position at the Swedish University of Agricultural Sciences (SLU). We would especieally like to thank Jenny Ekman, Abdulmajid Mahomoud and Margareta Elfving in the Biogeochemical Analyses Laboratory (BAL) from FEM of SLU for their supports to the sample analysis works. Finally, three anonymous reviewers' valuable comments are greatly appreciated.

Appendix A. Supplementary data

Supplementary data to this article can be found online at https://doi.org/10.1016/j.watres.2019.115217.

References

Aeschbacher, M., Graf, C., Schwarzenbach, R.P., Sander, M., 2012. Antioxidant properties of humic substances. Environ. Sci. Technol. 46, 4916–4925.
Aeschbacher, M., Sander, M., Schwarzenbach, R.P., 2010. Novel electrochemical approach to assess the redox properties of humic substances. Environ. Sci. Technol. 44, 87–93.
Alberts, J.J., Schindler, J.E., Miller, R.W., 1974. Elemental mercury evolution mediated by humic acid. Science 184, 895–896.
Allard, B., Arsenie, I., 1991. Abiotic reduction of mercury by humic substances in aquatic system-an important process for the mercury cycle. Water Air Soil Pollut. 56, 457–464.
Bauer, M., Heitmann, T., Macalady, D.L., Blodau, C., 2007. Electron transfer capacities and reaction kinetics of peat dissolved organic matter. Environ. Sci. Technol. 41, 139–145.
Bauer, I., Kappler, A., 2009. Rates and extent of reduction of Fe(II) compounds and O_2 by humic substances. Environ. Sci. Technol. 43, 4902–4908.
Blodau, C., Mayer, B., Peiffer, S., Moore, T.R., 2007. Support for an anaerobic sulfur cycle in two Canadian peatland soils. J. Geophys. Res. Biogeosci. 112, G2.
Blodau, C., Bauer, M., Regenspurg, S., Macalady, D., 2009. Electron accepting capacity of dissolved organic matter as determined by reaction with metallic zinc. Chem. Geol. 260, 186–195.
Cory, R.M., Crump, B.C., Dobkowski, J.A., Kling, G.W., 2013. Surface exposure to sunlight stimulates CO_2 release from permafrost soil carbon in the Arctic. Proc. Natl. Acad. Sci. 110, 3429–3434.
Cory, R.M., Ward, C.P., Crump, B.C., Kling, G.W., 2014. Sunlight controls water column processing of carbon in arctic fresh waters. Science 345, 925–928.
Daugherty, E.E., Gilbert, B., Nico, P.S., Borch, T., 2017. Complexation and redox buffering of iron(II) by dissolved organic matter. Environ. Sci. Technol. 51, 11096–11104.
Downing, B.D., Boss, E., Bergamaschi, B.A., Fleck, J.A., Lionberger, M.A., Ganju, N.K., Schoellhamer, D.H., Fujii, R., 2009. Quantifying fluxes and characterizing compositional changes of dissolved organic matter in aquatic systems in situ using combined acoustic and optical measurements. Limnol Oceanogr. Methods 7, 119–131.
Fellman, J.B., Hood, E., Spencer, R.G.M., 2010. Fluorescence spectroscopy opens new windows into dissolved organic matter dynamics in freshwater ecosystems: a review. Limnol. Oceanogr. 55, 2452–2462.
Feng, X., Meng, B., Yan, H., Fu, X., Yao, H., Shang, L., 2018. Biogeochemical Cycle of Mercury in Reservoir Systems in Wujiang River Basin, Southwest China. Springer Nature, Singapore.
Fichot, C.G., Kaiser, K., Hooker, S.B., Amon, R.M.W., Babin, M., Bélanger, S., Walker, S.A., Benner, R., 2013. Pan-Arctic distributions of continental runoff in the Arctic Ocean. Sci. Rep. 3, 1053.
Fichot, G., Benner, R., 2012. The spectral slope coefficient of chromophoric dissolved organic matter ($S_{275-295}$) as a tracer of terrigenous dissolved organic carbon in river-influenced ocean margins. Limnol. Oceanogr. 57 (5), 1453–1466.
Gao, C., Sander, M., Agethen, S., Knorr, K.-H., 2019. Electron accepting capacity of dissolved and particulate organic matter control CO_2 and CH_4 formation in peat soils. Geochem. Cosmochim. Acta 245, 266–277.
Gu, B., Yan, H., Zhou, P., Watson, D.B., 2005. Natural humics impact uranium bioreduction and oxidation. Environ. Sci. Technol. 39, 5268–5275.
Gu, B., Bian, Y., Miller, C.L., Dong, W., Jiang, X., Liang, L., 2011. Mercury reduction and complexation by natural organic matter in anoxic environments. Proc. Natl. Acad. Sci. 108, 1479–1483.
Gu, B., Chen, J., 2003. Enhanced microbial reduction of Cr(VI) and U(VI) by different natural organic matter fractions. Geochem. Cosmochim. Acta 67, 3575–3582.
Hansen, A.M., Kraus, T.E.C., Pellerin, B.A., Fleck, J.A., Downing, B.D., Bergamaschi, B.A., 2016. Optical properties of dissolved organic matter (DOM): effects of biological and photolytic degradation. Limnol. Oceanogr. 61, 1015–1032.
Helburn, R.S., MacCarthy, P., 1994. Determination of some redox properties of humic acid y alkaline ferricyanide titration. Anal. Chim. Acta 295, 263–272.
Helms, J.R., Stubbins, A., Ritchie, J.D., Minor, E.C., Kieber, D.J., Mopper, K., 2008. Absorption spectral slopes and slope ratios as indicators of molecular weight, source, and photobleaching of chromophoric dissolved organic matter. Limnol. Oceanogr. 53, 955–969.
Hernández-Montoya, V., Alvarez, L.H., Montes-Morán, M.A., Cervantes, F.J., 2012. Reduction of quinone and non-quinone redox functional groups in different humic acid samples by *Geobacter sulfurreducens*. Geoderma 183–184, 25–31.
Huguet, A., Vacher, L., Relexans, S., Saubusse, S., Froidefond, J.M., Parlanti, E., 2009. Properties of fluorescent dissolved organic matter in the Gironde Estuary. Org. Geochem. 40, 706–719.
Jiang, J., Kappler, A., 2008. Kinetics of microbial and chemical reduction of humic substances: implications for electron shuttling. Environ. Sci. Technol. 42, 3563–3569.
Jiang, T., Chen, X.S., Wang, D.Y., Liang, J., Bai, W.Y., Zhang, C., Wang, Q.L., Wei, S.Q., 2018a. Dynamics of dissolved organic matter (DOM) in a typical inland lake of the Three Gorges Reservoir area: fluorescent properties and their implications for dissolved mercury species. J. Environ. Manag. 206, 418–429.
Jiang, T., Bravo, A.G., Skyllberg, U., Björn, E., Wang, D.Y., Yan, H.Y., Green, N.W., 2018b. Influences of dissolved organic matter (DOM) characteristics on dissolved mercury (Hg) species composition in sediment porewater of lakes from southwest China. Water Res. 146, 146–158.
Jiang, T., Skyllberg, U., Wei, S.Q., Wang, D.Y., Lu, S., Jiang, Z.M., Flanagan, D.C., 2015. Modeling of the structure-specific kinetics of abiotic, dark reduction of Hg(II) complexed by O/N and S functional groups in humic acids while accounting for time-dependent structural rearrangement. Geochem. Cosmochim. Acta 154, 151–167.
Jiang, T., Wei, S.Q., Flanagan, D.C., Li, M.J., Li, X.M., Wang, Q., Luo, C., 2014. Effect of abiotic factors on the mercury reduction process by humic acids in aqueous systems. Pedosphere 24, 125–136.
Jiskra, M., Wiederhold, J.G., Skyllberg, U., Kronberg, R.-M., Hajdas, I., Kretzschmar, R., 2015. Mercury deposition and re-emission pathways in boreal forest soils investigated with Hg isotope signatures. Environ. Sci. Technol. 49, 7188–7196.
Jonsson, S., Andersson, A., Nilsson, M.B., Skyllberg, U., Lundberg, E., Schaefer, J.K., Åkerblom, S., Björn, E., 2017. Terrestrial discharges mediate trophic shifts and enhance methylmercury accumulation in estuarine biota. Sci. Adv. 2, e1601239.
Kaiser, K., Canedo-Oropeza, M., McMahon, R., Amon, R.M.W., 2017. Origins and transformations of dissolved organic matter in large Arctic rivers. Sci. Rep. 7, 13064.
Kappler, A., Haderlein, S.B., 2003. Natural organic matter as reductant for chlorinated aliphatic pollutants. Environ. Sci. Technol. 37, 2714–2719.
Kappler, A., Benz, M., Schink, B., Brune, A., 2004. Electron shuttling via humic acids in microbial iron(III) reduction in a freshwater sediment. FEMS Microbiol. Ecol. 47, 85–92.
Karlsson, J., Giesler, R., 2008. Global change and the high-latitude environment: high latitude terrestrial and freshwater ecosystems: interactions and response to environmental change; Abisko, Sweden, 11–14 september 2007. Eos 89, 97–97.
Kellerman, A.M., Dittmar, T., Kothawala, D.N., Tranvik, L.J., 2014. Chemodiversity of dissolved organic matter in lakes driven by climate and hydrology. Nat. Commun. 5, 3804.
Knorr, K.H., Blodau, C., 2009. Impact of experimental drought and rewetting on redox transformations and methanogenesis in mesocosms of a northern fen soil. Soil Biol. Biochem. 41, 1187–1198.
Kokic, J., Wallin, M.B., Chmiel, H.E., Denfeld, B.A., Sobek, S., 2015. Carbon dioxide evasion from headwater systems strongly contributes to the total export of carbon from a small boreal lake catchment. J. Geophys. Res. Biogeosci. 120, 2014JG002706.
Kothawala, D.N., Stedmon, C.A., Müller, R.A., Weyhenmeyer, G.A., Köhler, S.J., Tranvik, L.J., 2014. Controls of dissolved organic matter quality: evidence from a large-scale boreal lake survey. Glob. Chang. Biol. 20, 1101–1114.
Larouche, J.R., Abbott, B.W., Bowden, W.B., Jones, J.B., 2015. The role of watershed characteristics, permafrost thaw, and wildfire on dissolved organic carbon biodegradability and water chemistry in Arctic headwater streams. Biogeosciences 12, 4221–4233.
Larson, J.H., Frost, P.C., Xenopoulos, M.A., Williams, C.J., Morales-Williams, A.M., Vallazza, J.M., Nelson, J.C., Richardson, W.B., 2014. Relationships between land cover and dissolved organic matter change along the river to lake transition. Ecosystems 17, 1413–1425.
Lee, S., Roh, Y., Kim, K.-W., 2019. Influence of chloride ions on the reduction of mercury species in the presence of dissolved organic matter. Environ. Geochem. Health 41, 71–79.
Lescord, G.L., Emilson, E.J.S., Johnston, T.A., Branfireun, B.A., Gunn, J.M., 2018. Optical properties of dissolved organic matter and their relation to mercury concentrations in water and biota across a remote freshwater drainage basin. Environ. Sci. Technol. 52, 3344–3353.
Lovley, D.R., Blunt-Harris, E.L., 1999. Role of humic-bound iron as an electron transfer agent in dissimilatory Fe(III) reduction. Appl. Environ. Microbiol. 65, 4252–4254.
Lovley, D.R., Coates, J.D., Blunt-Harris, E.L., Phillips, E.J.P., Woodward, J.C., 1996. Humic substances as electron acceptors for microbial respiration. Nature 382, 445–448.

Macalady, D.L., Walton-Day, K., 2011. Redox chemistry and natural organic matter (NOM): geochemists' dream, analytical chemists' nightmare (Chapter 5). In: Tratnyek, P.G., Grundl, T.J., Haderlein, S.B. (Eds.), Aquatic Redox Chemistry (ACS Symposium Series 1071). American Chemical Society, Washington, DC.
Mann, P.J., Spencer, R.G.M., Hernes, P.J., Six, J., Aiken, G.R., Tank, S.E., McClelland, J.W., Butler, K.D., Dyda, R.Y., Holmes, R.M., 2016. Pan-Arctic trends in terrestrial dissolved organic matter from optical measurements. Front. Earth Sci. 4, 25.
Maurer, F., Christl, I., Fulda, B., Voegelin, A., Kretzschmar, R., 2013. Copper redox transformation and complexation by reduced and oxidized soil humic acid. 2. Potentiometric titrations and dialysis cell experiments. Environ. Sci. Technol. 47, 10912–10921.
Maurer, F., Christl, I., Kretzschmar, R., 2010. Reduction and reoxidation of humic acid: influence on spectroscopic properties and proton binding. Environ. Sci. Technol. 44, 5787–5792.
McKnight, D.M., Aiken, G.R., Smith, R.L., 1991. Aquatic fulvic acids in microbially based ecosystems: results from two desert lakes in Antarctica. Limnol. Oceanogr. 36, 998–1006.
McKnight, D.M., Boyer, E.W., Westerhoff, P.K., Doran, P.T., Kulbe, T., Anderson, D.T., 2001. Spectrofluorometric characterization of dissolved organic matter for identification of precursor material and aromaticity. Limnol. Oceanogr. 46, 38–48.
Nurmi, J.T., Tratnyek, P.G., 2011. Electrochemistry of natural organic matter (Chapter 7). In: Tratnyek, P.G., Grundl, T.J., Haderlein, S.B. (Eds.), Aquatic Redox Chemistry (ACS Symposium Series 1071). American Chemical Society, Washington, DC.
O'Donnell, J.A., Aiken, G.R., Swanson, D.K., Panda, S., Butler, K.D., Baltensperger, A.P., 2016. Dissolved organic matter composition of Arctic rivers: linking permafrost and parent material to riverine carbon. Glob. Biogeochem. Cycles 30, 1811–1826.
Osburn, C.L., Anderson, N.J., Stedmon, C.A., Giles, M.E., Whiteford, E.J., McGenity, T.J., Dumbrell, A.J., Underwood, G.J.C., 2017. Shifts in the source and composition of dissolved organic matter in Southwest Greenland lakes along a regional hydroclimate gradient. J. Geophys. Res. Biogeosci. 122, 3431–3445.
Osterwalder, S., Bishop, K., Alewell, C., Fritsche, J., Laudon, J., Åkerblom, S., Nilsson, M.B., 2017. Mercury evasion from a boreal peatland shortens the timeline for recovery from legacy pollution. Sci. Rep. 7, 16022.
Perdue, E.M., Koprivnjak, J.-F., 2007. Using the C/N ratio to estimate terrigenous inputs of organic matter to aquatic environment. Estuar. Coast Shelf Sci. 73, 65–72.
Peretyazhko, T., Sposito, G., 2006. Reducing capacity of terrestrial humic acids. Geoderma 137, 140–146.
Pham, N.A., Rose, A.L., Waite, D.T., 2012. Kinetic of Cu(II) reduction by natural organic matter. J. Phys. Chem. A 116, 6590–6599.
Poulin, B.A., Ryan, J.N., Aiken, G.R., 2014. Effects of iron on optical properties of dissolved organic matter. Environ. Sci. Technol. 48, 10098–10106.
Poulin, B.A., Ryan, J.N., Nagy, K.L., Stubbins, A., Dittmar, T., Orem, W., Krabbenhoft, D.P., Aiken, G.R., 2017. Spatial dependence of reduced sulfur in Everglades dissolved organic matter controlled by sulfate enrichment. Environ. Sci. Technol. 51, 3630–3639.
Ratasuk, N., Nanny, M.A., 2007. Characterization and quantification of reversible redox sites in humic substances. Environ. Sci. Technol. 41, 7844–7850.
Ripszam, M., Paczkowska, J., Figueria, J., Veenaas, C., Haglund, P., 2015. Dissolved organic carbon quality and sorption of organic pollutants in the Baltic Sea in light of future climate change. Environ. Sci. Technol. 49, 1445–1452.
Roden, E.E., Kappler, A., Bauer, I., Jiang, J., Paul, A., Stoesser, R., Konishi, H., Xu, H., 2010. Extracellular electron transfer through microbial reduction of solid-phase humic substances. Nat. Geosci. 3, 417–421.
Schartup, A.T., Balcom, P.H., Soerensen, A.L., Gosnell, K.J., Calder, R.S.D., Mason, R.P., Sunderland, E.M., 2015a. Freshwater discharges drive high levels of methylmercury in Arctic marine biota. Proc. Natl. Acad. Sci. 112, 11789–11794.
Schartup, A.T., Ndu, U., Balcom, P.H., Mason, R.P., Sunderland, E.M., 2015b. Contrasting effects of marine and terrestrially derived dissolved organic matter on mercury speciation and bioavailability in seawater. Environ. Sci. Technol. 49, 5965–5972.
Schuster, P.F., Schaefer, K.M., Aiken, G.R., Antweiler, R.C., Dewild, J.F., Gryziec, J.D., Gusmeroli, A., Hugelius, G., Jafarov, E., Krabbenhoft, D.P., Liu, L., Herman-Mercer, N., Mu, C., Roth, D.A., Schaefer, T., Striegl, R.G., Wickland, K.P., Zhang, T., 2018. Permafrost stores a globally significant amount of mercury. Geophys. Res. Lett. 45, 1463–1471.
Schuur, E.A.G., McGuire, A.D., Schädel, C., Grosse, G., Harden, J.W., Hayes, D.J., Hugelius, G., Koven, C.D., Kubry, P., Lawrence, D.M., Natali, S.M., Olefeldt, D., Romanovsky, V.E., Schaefer, K., Turetsky, M.R., Treat, C.C., Vonk, J.E., 2015. Climate change and the permafrost carbon feedback. Nature 520, 171–179.
Scott, D.T., McKnight, D.M., Blunt-Harris, E.L., Kolesar, S.E., Lovley, D.R., 1998. Quinone moieties act as electron acceptors in the reduction of humic substances by humic-reducing microorganisms. Environ. Sci. Technol. 32, 2984–2989.
Sharpless, C.M., Aeschbacher, M., Page, S.E., Wenk, J., Sander, M., McNeill, K., 2014. Photooxidation-induced changes in optical, electrochemical, and photochemical properties of humic substances. Environ. Sci. Technol. 48, 2688–2696.
Shcherbina, N.S., Perminova, I.V., Kalmykov, S.N., Kovalenko, A.N., Haire, R.G., Novikov, A.P., 2007. Redox and complexation interactions of neptunium (V) with quinonoid-enriched humic derivatives. Environ. Sci. Technol. 41, 7010–7015.
Shen, Y., Benner, R., Robbins, L.L., Wynn, J.G., 2016. Sources, distributions, and dynamics of dissolved organic matter in the Canada and Makarovs basins. Front. Mar. Sci. 3, 198.
Skyllberg, U., 2008. Competition among thiols and inorganic sulfides and polysulfides for Hg and MeHg in wetland soils and sediments under suboxic conditions: illumination of controversies and implications for MeHg net production. J. Geophys. Res. Biogeosci. 113, G2.
Sobek, S., Tranvik, L.J., Prairie, Y.T., Kortelainen, P., Cole, J.J., 2007. Patterns and regulation of dissolved organic carbon: an analysis of 7500 widely distributed lakes. Limnol. Oceanogr. 52, 1208–1219.
Sposito, G., 2011. Electron shuttling by natural organic matter: twenty years after (Chapter 6). In: Tratnyek, P.G., Grundl, T.J., Haderlein, S.B. (Eds.), Aquatic Redox Chemistry (ACS Symposium Series 1071). American Chemical Society, Washington, DC.
Stevenson, F.J., 1994. Humus Chemistry: Genesis, Composition, Reactions, second ed. John Wiley and Sons, New York.
Stookey, L.L., 1970. Ferrozine: a new spectrophotometric reagent for iron. Anal. Chem. 42, 779–781.
Struyk, Z., Sposito, G., 2001. Redox properties of standard humic acids. Geoderma 102, 329–346.
Viollier, E., Inglett, P.W., Hunter, K., Roychoudhury, A.N., Cappellen, P.V., 2000. The ferrozine method revisited: Fe(II)/Fe(III) determination in natural waters. Appl. Geochem. 15, 785–790.
Vonk, J.E., Tank, S.E., Bowden, W.B., Laurion, I., Vincent, W.F., Alekseychik, P., Amyot, M., Billet, M.F., Canário, J., Cory, R.M., Deshpande, B.N., Helbig, M., Jammet, M., Karlsson, J., Larouche, J., MacMillan, G., Rautio, M., Walter-Anthony, K.M., Wickland, K.P., 2015. Reviews and syntheses: effects of permafrost thaw on Arctic aquatic ecosystems. Biogeosciences 12, 7129–7167.
Walpen, N., Getzinger, G.J., Schroth, M.H., Sander, M., 2018. Electron-donating phenolic and electron-accepting quinone moieties in peat dissolved organic matter: quantities and redox transformations in the context of peat biogeochemistry. Environ. Sci. Technol. 52, 5236–5245.
Wei-Hass, M.L., Hageman, K.J., Chin, Y.-P., 2014. Partitioning of polybrominated diphenyl ethers to dissolved organic matter isolated from Arctic surface waters. Environ. Sci. Technol. 48, 4852–4859.
Weishaar, J.L., Aiken, G.R., Bergamaschi, B.A., Fram, M.S., Fujii, R., Mopper, K., 2003. Evaluation of specific ultraviolet absorbance as an indicator of the chemical composition and reactivity of dissolved organic carbon. Environ. Sci. Technol. 37, 4702–4708.
Wilson, H.F., Xenopoulos, M.A., 2009. Effects of agricultural land use on the composition of fluvial dissolved organic matter. Nat. Geosci. 2, 37–41.
Xiao, Y.-H., Sara-Aho, T., Hartikainen, H., Vähätalo, A.V., 2013. Contribution of ferric iron to light absorption by chromophoric dissolved organic matter. Limnol. Oceanogr. 58, 653–662.
Xiao, Y.-H., Räike, A., Hartikainen, H., Vähätalo, A.V., 2015. Iron as a source of color in river waters. Sci. Total Environ. 536, 914–923.
Xie, L., Shang, C., 2005. Role of humic acid and quinone model compounds in bromate reduction by zerovalent iron. Environ. Sci. Technol. 39, 1092–1100.
Yang, L., Hur, J., 2014. Critical evaluation of spectroscopic indices for organic matter source tracing via end member mixing analysis based on two contrasting sources. Water Res. 59, 80–89.
Yu, Z.-G., Peiffer, S., Göttlicher, J., Knorr, K.-H., 2015. Electron transfer budgets and kinetics of abiotic oxidation and incorporation of aqueous sulfide by dissolved organic matter. Environ. Sci. Technol. 49, 5441–5449.
Zhao, L., Anderson, C.W.N., Qiu, G., Meng, B., Wang, D., Feng, X., 2016. Mercury methylation in paddy soil: source and distribution of mercury species at a Hg mining area, Guizhou Province, China. Biogeosciences 13, 2429–2440.
Zheng, W., Liang, L., Gu, B., 2012. Mercury reduction and oxidation by reduced natural organic matter in anoxic environments. Environ. Sci. Technol. 46, 292–299.
Zhu, W., Lin, C.-J., Wang, X., Sommar, J., Fu, X., Feng, X., 2016. Global observations and modelling of atmosphere-surface exchange of elemental mercury: a critical review. Atmos. Chem. Phys. 16, 4451–4480.
Zhu, W., Song, Y., Adediran, G.A., Jiang, T., Reis, A.T., Pereira, E., Skyllberg, U., Björn, E., 2018. Mercury transformations in resuspended contaminated sediment controlled by redox conditions, chemical speciation and sources of organic matter. Geochem. Cosmochim. Acta 220, 158–179.